Liquid Crystals
Publication details, including instructions for authors and subscription information:
http://www.informaworld.com/smpp/title~content=t713926090

Effects of organomontmorillonite concentration on the structure formation of nanocomposites with 5CB liquid crystal

T. Bezrodna[a]; I. Chashechnikova[a]; G. Puchkovska[a]; A. Tolochko[a]; E. Shaydyuk[a]; N. Lebovka[b]; J. Baran[c]; M. Drozd[c]; H. Ratajczak[c]
[a] Institute of Physics, National Academy of Sciences Ukraine, Kyiv 03022, Ukraine [b] Institute of Biocolloidal Chemistry, National Academy of Sciences Ukraine, 42 Vernadskii Prosp., Ukraine [c] Institute of Low Temperature and Structure Research, Polish Academy of Sciences, *50-950 Wroclaw*, *Poland*,

To cite this Article Bezrodna, T. , Chashechnikova, I. , Puchkovska, G. , Tolochko, A. , Shaydyuk, E. , Lebovka, N. , Baran, J. , Drozd, M. and Ratajczak, H.(2006) 'Effects of organomontmorillonite concentration on the structure formation of nanocomposites with 5CB liquid crystal', Liquid Crystals, 33: 10, 1113 — 1119
To link to this Article: DOI: 10.1080/02678290601032646
URL: http://dx.doi.org/10.1080/02678290601032646

Liquid Crystals, Vol. 33, No. 10, October 2006, 1113–1119

Effects of organomontmorillonite concentration on the structure formation of nanocomposites with 5CB liquid crystal

T. BEZRODNA†, I. CHASHECHNIKOVA†, G. PUCHKOVSKA*†, A. TOLOCHKO†, E. SHAYDYUK†, N. LEBOVKA‡, J. BARAN§, M. DROZD§ and H. RATAJCZAK§

†Institute of Physics, National Academy of Sciences Ukraine, 46 Nauki Prosp, Kyiv 03022, Ukraine
‡Institute of Biocolloidal Chemistry, National Academy of Sciences Ukraine, 42 Vernadskii Prosp., Kyiv 03142, Ukraine
§Institute of Low Temperature and Structure Research, Polish Academy of Sciences, *50-950 Wroclaw*, *Poland*

(*Received 7 June 2006; accepted 7 August 2006*)

Organoclay – 4–pentyl–4'–cyanobiphenyl (5CB) liquid crystal heterocomposites have been investigated using X-ray diffraction, IR-spectroscopy, polarizing optical microscopy (POM) and differential scanning calorimetry (DSC). Montmorillonite clay modified by dioctadecyldimethylammonium chloride was used as an inorganic component, and is hereinafter referred to as B3. Its concentration varied from 2 to 8 wt % in the composite materials. This modification of the clay results in a significant expansion of its interplanar spacing, into which 5CB dimers can penetrate during synthesis of the composite. It was found that the concentration dependence of the composite structure formation is dramatic. The most homogeneous system is formed at the clay concentration, C_{B3}=4.5%, as a result of Van der Waals interactions in this composite.

1. Introduction

Heterosystems consisting of an organic substance and inorganic nanoparticles are being intensively studied by various physical methods, due to the wide applications of such composites in modern nanotechnology. In particular, it has been found that their physico-chemical properties depend on the concentration of nanoparticles and the surface chemical interface interactions of the inorganic component in the organic medium. For example, the electro-optical properties and structural peculiarities of aerosil suspensions have been investigated over a range of concentration from 2 to 15 wt % in 5CB [1, 2]. A maximum optical memory effect was observed in the case of composites with 3 wt % of A-300 aerosil, with 4% of alumoaerosil, or with 5% of titanium aerosil. The presence of aerosil particles does not change the nematic to isotropic phase transition temperature (PTT) of 5CB; however, the incorporation of polymethylmethacrylate (PMMA) spherical particles in the LC decreases its PTT with increase in polymer concentration [3]. The dielectrical properties of heterosystems based on E7 LC with varying content (from 0 to 8.6 wt %) of poly(methylmethacrylate-co-divinylbenzene) colloidal particles have been investigated [4]; it was found that the conductivity in these composites grows with increasing concentration of solid particles over a wide temperature range.

Layered clay minerals are also very efficient as inorganic components of the composites. This is due mainly to their large specific surface, high dispersability in suspensions, and the anisometric structure of particles. However, their surface is organophobic in its initial state, and in order to make the surface organophilic, clay minerals are modified with organic surfactants. In particular, the structure and thermoelastic properties of nanocomposites consisting of organo-modified montmorillonite (MMT) and chloroprene (or butadienestyrene) caoutchouc have been investigated in [5]. Optimum mechanico-relaxation properties were found in composites with 4–5 wt % of the organoclay, because an 'infinite cluster' is formed in such elastomeric nanocomposites at this concentration.

The effects of organomodified bentonite concentration on the rheological properties of heterosystems based on this mineral in a matrix of liquid hydrocarbons or epoxy resins have also been studied [6, 7]. The experimental data demonstrated an abrupt increase in composite viscosity when the bentonite concentration reached a critical value. It has also been shown that the modification of Na-MMT with dioctadecyldimethylammonium chloride (DODM) leads to the appearance of electro-optical effects (in particular, a memory effect) in the 5CB–MMT composites, because of near-surface interactions at the phase separation boundary, [8].

*Corresponding author. Email: puchkov@iop.kiev.ua

Liquid Crystals
ISSN 0267-8292 print/ISSN 1366-5855 online © 2006 Taylor & Francis
http://www.tandf.co.uk/journals
DOI: 10.1080/02678290601032646

The aim of the present work is the investigation of MMT-DODM concentration effects on structure formation in composites with 5CB and on the character of interactions between the components in these heterosystems.

2. Materials and experimental methods

The nematic LC 5CB, having its solid crystal – nematic LC PTT at 295 K, and nematic LC–isotropic liquid PTT at 308.3 K, was used as LC matrix in the composites. In the nematic and isotropic phases 5CB molecules form dipole – dipole bound dimers about 2.3 nm long and 0.5 nm thick [9]. The inorganic component of these heterosystems consisted of particles of the layered clay MMT mineral (Askan deposit) modified with DODM. The profile of clay mineral samples, the modification methods of the Na-form MMT by a DODM surfactant and the synthesis of the composites have previously been described in detail [8]. The 5CB–B3 heterosystems, containing 2, 3, 4.5, 6 and 8 wt % of B3 are used in this study.

In order to study the structure of clay minerals and the 5CB–B3 composites, and also the effects of B3 concentration on the structure of the heterosystems and interface interactions, the experimental methods of small-angle X-ray diffraction (XRD), polarizing opticalmicroscopy (POM), differential scanning calorimetry (DSC), and IR-spectroscopy were used. XRD measurements were performed using a small angle diffractometer AMUR with a slit collimation system. CuK_{α}-radiation from a 1.2 kw X-ray tube with focus size of $0.4 \times 8\,mm^2$, and Ni-foil monochromator were used. The distances between source and sample, and between sample and detector were 500 and 350 mm, respectively. Scattered radiation reached the detector via a vacuum chamber. The intensity of scattered radiation was measured in the 2θ angle range from 0.1° to 8° with steps of 0.02°.

The samples of dry Na-MMT and B3 were studied in a flat cell with beryllium windows; the cell thickness was 0.5 mm. The nanocomposite suspensions were placed into a thin wall Lindemann capillary, 0.7 mm in diameter; this was mounted in a temperature-controlled camera, equipped with a magnet for obtaining oriented samples during cooling from the isotropic phase. The temperature was measured with a copper–constantan thermocouple with an accuracy of 0.2°C. The PRIMUS comprehensive program complex was applied for the treatment of experimental results [10]. Modelling of an optimal conformation for the modifier molecules was carried out by the UFF method with the use of ArgusLab 4.0.1[11].

Photomicrographs of all nanocomposites with different B3 concentrations in polarized light were obtained on a Carl Zeiss Peraval Interphako microscope with a heating table, the magnification was × 500. DSC data, i.e. the phase transition temperatures and phase transition enthalpies, were measured with a Perkin-Elmer DSC7 instrument under heating and cooling regimes in the range 20–70°C at a heating rate of $20\,K\,min^{-1}$. Al pans were used. Room temperature IR spectra were measured in the spectral range of 380–$4000\,cm^{-1}$ on a Bruker FTIR spectrometer (system IFS-88) at a resolution of $1\,cm^{-1}$ and with 64 scans. The spectra of clay mineral powders were measured in Nujol and Fluorolube, and suspensions of the 5CB–B3 composites were placed between KBr windows, the thickness of the samples was 10–15 μm.

3. Results and discussion

3.1. *XRD experiments*

Figure 1 (*a*) shows XRD data for the Na-MMT and B3 dry powders, and for 5CB. The first sample is seen to be typical of the sodium form MMT, of layered periodicity with d=1.24 nm. In the case of the modified B3 sample two peaks, corresponding to d_1=3.6 nm and d_2=1.9 nm interplane distances, are clearly seen. In our opinion, this is due to the different packing of modifier molecules, in relation to the surface planes of the clay interlayer spaces; i.e. under an angle close to 90° and nearly parallel orientation, since the length of a DODM molecule is about 2.5 nm, and its diameter is about 0.55 nm, values which approximately correspond with the differences in d between Na-MMT and B3 clays.

For the 5CB–B3 nanocomposites with the B3 concentrations of 2, 3, 4.5, 6, 8 wt %, an increase of 0.6 nm in the d_1 period is observed, figure 1 (*b*). This is probably due to the penetration of 5CB dimers into the

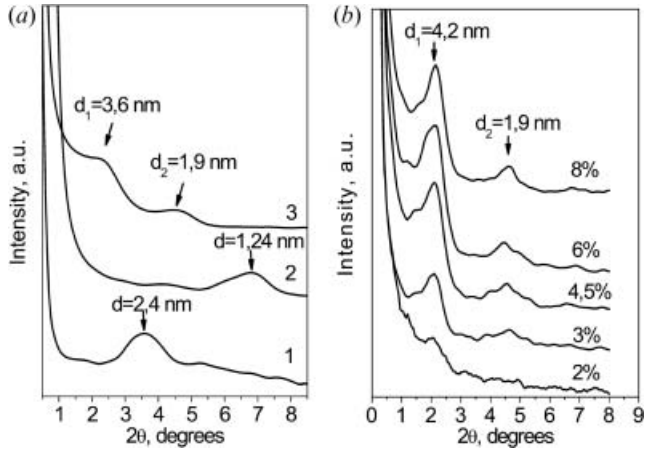

Figure 1. Small angle XRD- patterns of (*a*) 1, bulk 5CB; 2, dry powder Na-MMT clay; 3, dry powder B3 clay; (*b*) 5CB–B3 nanocomposites with C_{B3}=2, 3, 4.5, 6, 8 wt %.

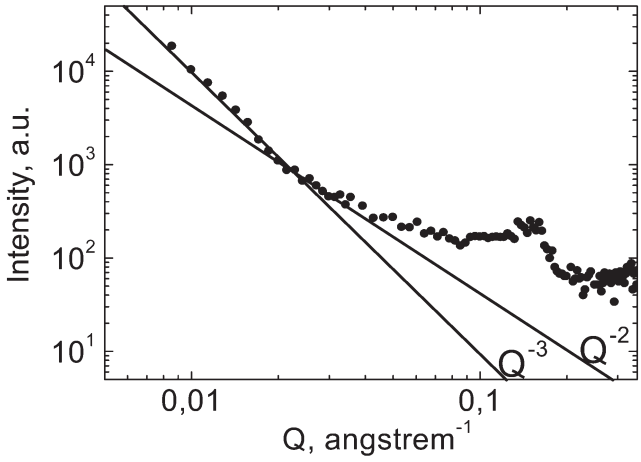

Figure 2. Double logarithm plot of XRD intensity in the scattering vector range $Q<0.1\,\text{Å}^{-1}$ for 4.5% B3 in 5CB (dots) and Q^{-n} fits (solid line).

inner space between the plates in a gallery of the organoclay, since the dimer diameter is ~0.5 nm; the d_2 value does not change. The 5CB periodicity period is observed at 2.4 nm, which corresponds approximately to the length of 5CB dimers. Curves in figure 1 (*b*) were corrected, taking account of 5CB diffraction.

The measurement of the intensity I as a function of the scattering vector, Q, in the region $0.01<Q<0.03\,\text{Å}^{-1}$ leads to the conclusion that the size of particles in the 5CB–B3 composites exceeds the size of a single clay plate. As seen from figure 2, in the case of 4.5% B3 concentration, intensity extrapolation towards the smallest values of Q results in an exact dependence $I\sim Q^{-3}$, which is characteristic for fractal systems [12]. In other words, the formation of a spatial network by the clay particles is possible in this system.

When $0.03<Q<0.05\,\text{Å}^{-1}$, an $I\sim Q^{-2}$ relation is observed, probably because of the presence of chaotically located disk-like plates. The latter are single clay particles and stacks of several particles. A similar pattern is observed for samples with a concentration of 3%. For higher concentrations the deviation from Q^{-3} dependence increases, and large agglomerates can be formed. Thus, it may be concluded, that in the 5CB–B3 system the optimum structure formation occurs under the clay concentrations of 3–4.5%.

3.2. *POM investigations*

Polarized light photomicrographs, obtained for the 5CB–B3 composites with organoclay concentrations of 2–8%, are shown in figure 3. At C_{B3} of 2%, inhomogeneous distribution of solid particles in the LC and large areas of pure 5CB are observed—dark coloured fragments in figure 3 (*a*). On increasing C_{B3}, the homogeneity of particle distribution in the matrix also increases, and a uniform structure is obtained at $C_{B3}=4.5\%$, figure 3 (*c*). With further increase of the organoclay content, the enlargement of solid particles is observed because of their agglomeration. At higher B3 concentrations, up to $C_{B3}=8\%$, the particles become larger and the structure of the composite less homogeneous, see figures 3 (*d*, *e*). According to the XRD studies it is clear that the best structure formation of the 5CB–B3 occurs at $C_{B3}\sim4.5\%$.

3.3. *DSC measurements*

Figure 4 shows DSC curves of the 5CB–B3 composites with different concentrations of the clay mineral on heating, (*a*) and cooling, (*b*), at a rate of $20\,\text{K min}^{-1}$. The nematic – isotrope PTT, T_{NI}, for the composites of 2 and 3% B3 concentration, remains practically the same as for bulk 5CB (308.3 K). The increase of B3 concentration to 4.5% leads to a significant decrease of PTT (nearly at 4 K); at $C_{B3}=6\%$ this difference is approximately 2 K, with a further decrease for $C_{B3}=8\%$.

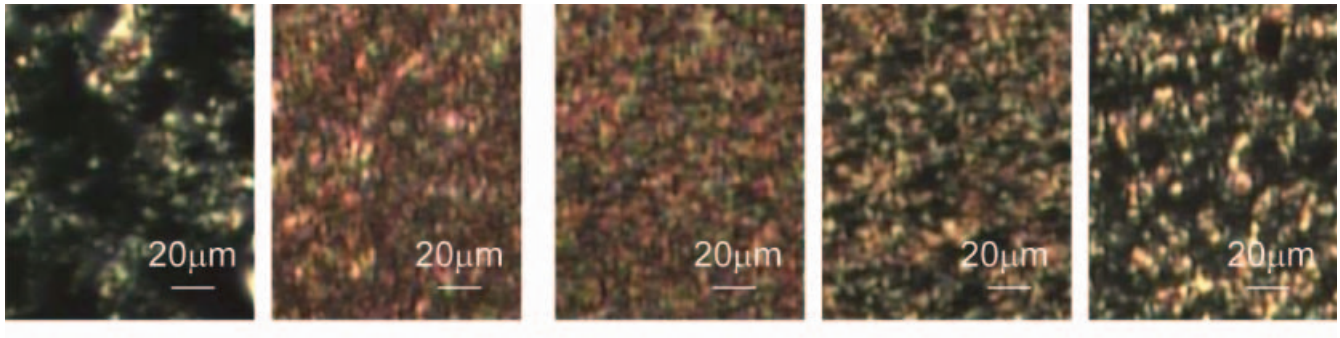

Figure 3. POM photomicrographs obtained with crossed polarizers for the 5CB–B3 composites: (*a*) $C_{B3}=2\%$, (*b*) $C_{B3}=3\%$, (*c*) $C_{B3}=4.5\%$, (*d*) $C_{B3}=6\%$, (*e*) $C_{B3}=8\%$.

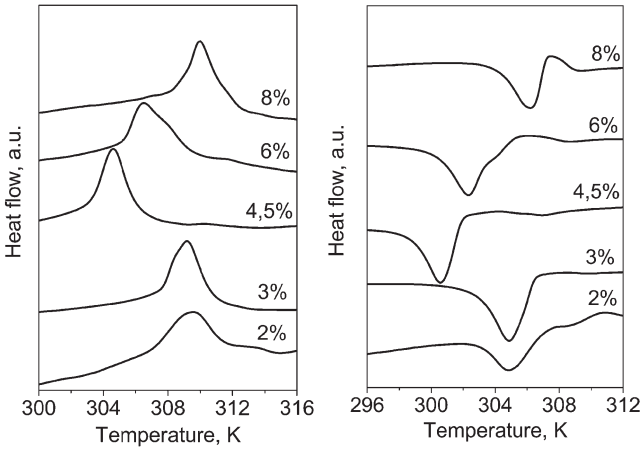

Figure 4. Thermograms of 5CB–B3 composites with different B3 concentrations, measured: (*a*) heating and (*b*) cooling.

It should be noted that the peak width of this phase transition is significantly larger for the composites with B3 concentrations of 2, 3, 6 and 8%, than for those for C_{B3}=4.5% and for bulk 5CB, this reflects the structure heterogeneity of these composites and the presence of spatial regions with different arrangements of LC structure under the various concentrations of B3.

In the case of the 5CB–MMT composite with C_{B3}=4.5%, the formation of a new homogeneous LC structure is seen, created in 5CB by a net of B3 anisometric solid particles, possessing large surfaces. On further increase of B3 concentration the difference in PTT between the 5CB–B3 composites and bulk 5CB lessens, which is probably due to particle agglomeration processes, with decrease of the real contact area with 5CB.

The heating – cooling hysteresis, figures 4 (*a*, *b*), observed for all composites may arise because the structure appearing under the influence of B3 particles does not totally disappear at the nematic – isotrope transition [13, 14].

These data are in good agreement with the results obtained from XRD and POM investigations (see § 3.1 and 3.2), which show the maximum structure formation in composites containing 4.5% of B3.

The observed extreme dependence of T_{NI} on C_{B3} is quite different from those measured for 5CB – aerosil systems [1, 2], where this dependence does not exist at all, and for LC–PMMA composites, where T_{NI} decreases as the concentration of solid particles increases [3]. The particles in those investigations had isometric shapes. Such a different influence of the solid component on the LC PTT can probably be explained by the different chemical nature of the particle surface, as well as their geometrical shape. These factors can significantly affect the character and strength of interactions between the heterocomposite elements.

In order to investigate the mechanisms of the above-mentioned interactions, which depend on B3 concentration in 5CB, we have carried out IR spectroscopic studies.

3.4. *IR-spectroscopy*

For the spectral analysis of concentration dependences, several IR bands were selected. Characteristic for the inorganic MMT component are bands at (a) 465 cm^{-1}, resulting from Si–O–Si, Al–O–Al deformation vibrations, (b) 1040 cm^{-1}, which is due to Si–O and Al–O stretching vibrations [15, 16]. Characteristic bands for the DODM and 5CB organic components are, those assigned to stretching vibrations of C≡N (2226 cm^{-1}), C–C (1606 cm^{-1}), C–H bonds in CH_2 (ν^a and ν^s), CH_3 (ν^a and ν^s), and benzene rings, ν^{ar}, and also to the in-plane β(CCH) deformations of benzene rings (1180 and 1186 cm^{-1}) [17]. These IR bands were selected because of the considerable sensitivity of their spectral parameters (frequency, intensity, half-width) to changes in intermolecular interactions, temperature, content, phase state; also because of a nearly total absence of overlap of these bands in the IR spectra of the inorganic and organic components, see figure 5.

For the first two bands (465 and 1040 cm^{-1}), characterizing the alumosilicate layers, a small spectral shift of their mass centres towards higher frequencies, and also some spectral narrowing of 1–1.5 cm^{-1} were observed. In order to simplify the analysis of the 465 cm^{-1} band spectral shape, all spectra were normalized to 1. This band has the largest mass-centre shift for the composite C_{B3}=2%, and the least spectral width in the case of C_{B3}=4.5%, figure 5 (*a*). In the spectral region of Si–O and Al–O stretching vibrations, figure 5 (*b*), the spectra were normalized on the 5CB band at 1006 cm^{-1}. A comparison of curves 7 and 3 shows a narrowing and a small shift of the band towards lower frequency. These observations indicate some compacting of the alumosilicate frame on a boundary with the organic matrix, in comparison with its state in the B3 powder. There is no simple linear concentration relationship for the spectral parameters of these bands.

The Q(C–C) and Q(C≡N) bands show even less changes, figure 5 (*c*). Again, their largest narrowing is seen for C_{B3}=4.5% (on ~1 cm^{-1}). The changes mentioned show the hindering of rotary movement of the 5CB dimers, relative to x-, y-axes (perpendicular to the *z*-axis), which contribute to the spectral width value of these bands. The peak positions of these bands are the same for all composites.

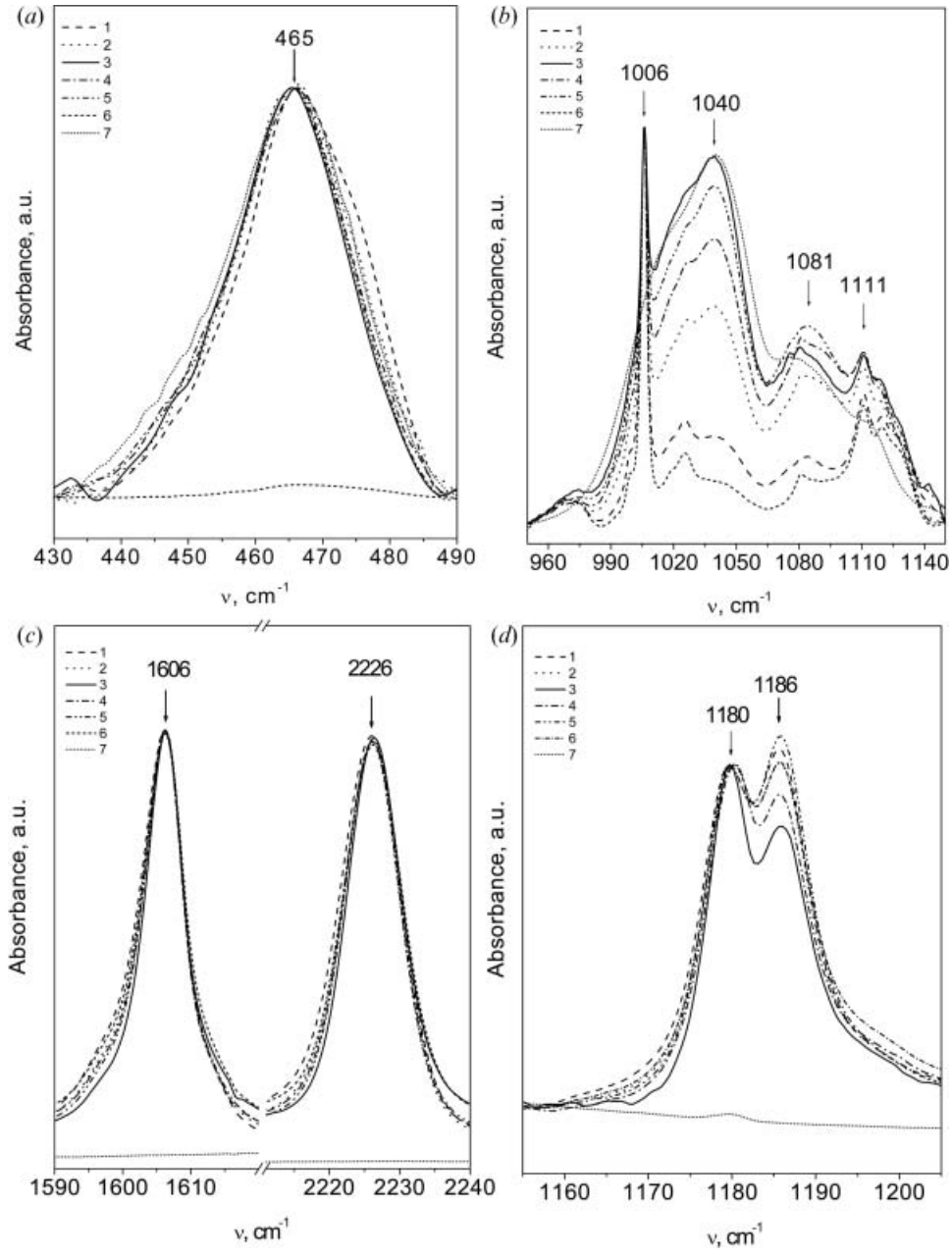

Figure 5. Sections of IR spectra for the 5CB–B3 composites: 1, C_{B3}=2%; 2, C_{B3}=3%; 3, C_{B3}=4.5%; 4, C_{B3}=6%; 5, C_{B3}=8%; 6, 5CB LC; 7 B3 organoclay. The spectral ranges correspond to: (*a*) β(O–Si–O), β(O–Al–O); (*b*) Q(Si–O), Q(Al–O); (*c*) Q(C–C), Q(C≡N); (*d*) biphenyl β(CCH) vibrations.

Figure 5 (*d*) shows the spectral bands at 1180 and 1186 cm^{-1}, resulting from the β(CCH) in-plane deformations of benzene rings. According to the calculations [17], the first is mainly arises from the vibrations of the benzene ring, nearest to a pentyl chain; the second one arises from the benzene ring near a cyano group. In this spectral region normalizing was performed on the 1180 cm^{-1} band. A significant extreme change is seen in the intensity ratio of these bands; the largest deviation is observed in the case of the 5CB–B3 composite with C_{B3}=4.5%.

The band observed at 2957 cm^{-1} is due to an asymmetrical CH_3 stretching ($\nu^a(CH_3)$) mode, the band at 2928 cm^{-1} to an asymmetrical CH_2 ($\nu^a(CH_2)$) mode; the band at 2857 cm^{-1} to symmetrical CH_2 stretching ($\nu^s(CH_2)$) vibrations, and the band at 2871 cm^{-1} – to a symmetrical CH_3 stretching ($\nu^s(CH_3)$) mode, figure 6 (*a*). According to our data, vibrations of exactly

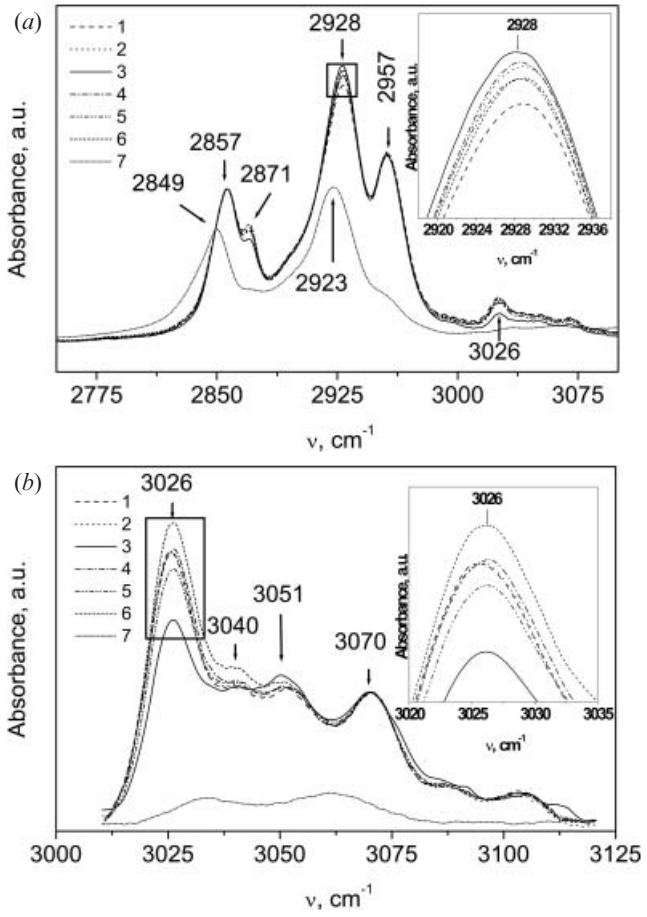

Figure 6. Sections of IR spectra for the 5CB–B3 composites: 1 – C_{B3}=2%, 2 – C_{B3}=3%, 3 – C_{B3}=4.5%, 4 – C_{B3}=6%, 5 – C_{B3}=8%; and 6–5CB LC, 7–B3 organoclay in the spectral regions, corresponding to the stretching q(CH) vibrations in: a) CH_2 and CH_3 –groups; b) benzene rings.

these groups on a periphery of 5CB molecules seem to be the most sensitive to the structural changes of 5CB–B3 composites with different B3 concentrations. As seen from figure 6(*a*), the peak positions of CH_2 stretching vibration modes for B3 powder (curve 7) and 5CB–B3 suspensions differ approximately by 6 cm^{-1}; the values for the corresponding CH_3 vibration bands differ by 3 cm^{-1}. The same stretching vibration frequency changes were observed during the melting of long chain aliphatic compounds (for example, paraffin $C_{33}H_{68}$ [18]), indicating in our case changes in the packing of DODM methylene chains and a decrease of chain interactions in the suspensions.

The locations of IR bands corresponding to CH-stretching vibrations of the 5CB molecule benzene ring, figure 6(*b*), do not depend on the B3 concentration in the composite. However, a decrease in intensity of the 3026 cm^{-1} band is observed in the presence of organoclay particles at all B3 concentrations, compared with the corresponding value for bulk 5CB. The lowest intensity of this band is seen in the case of the composite with C_{B3}=4.5%.

Concentration dependences of the intensity ratios for IR bands, arising from CH vibrations of the alkyl and phenyl groups of 5CB and DODM molecules, are presented in figure 7. All these characteristics are non-linear with an extreme at C_{B3}=4.5%. This relationship appears most clearly in the case of the band assigned to the stretching vibrations of aromatic CH-groups, figure 7 (curve 2), probably due to redistribution of the benzene ring π-electron density, resulting from a polarizing effect of the B3 anisometric particles. This figure also shows the concentration dependence of PTT, measured for the composites studied (curve 1), also having its extreme behaviour with a PTT minimum value for the composite with C_{B3}=4.5%.

Thus, from the IR spectral measurements it can be concluded that despite the relatively small values of the B3 and 5CB band spectral narrowing (~1–1.5 cm^{-1}), this effect indicates the mutual influence of the composite components, since it is observed for all the spectral bands considered. An additional confirmation of this conclusion is the similar character of B3 concentration dependence of spectral band widths and intensity ratios for CH-vibration bands in all hetero-systems. The largest spectral changes are always observed in the case of the 5CB–B3 composite with C_{B3}=4.5%, due to hugely significant interactions exactly in this heterogeneous system. The IR spectral results obtained correlate well with the DSC data, where the maximum decrease in the 5CB PTT is in the 5CB–B3 sample with C_{B3}=4.5%, figure 7, and also with the POM results, figure 3.

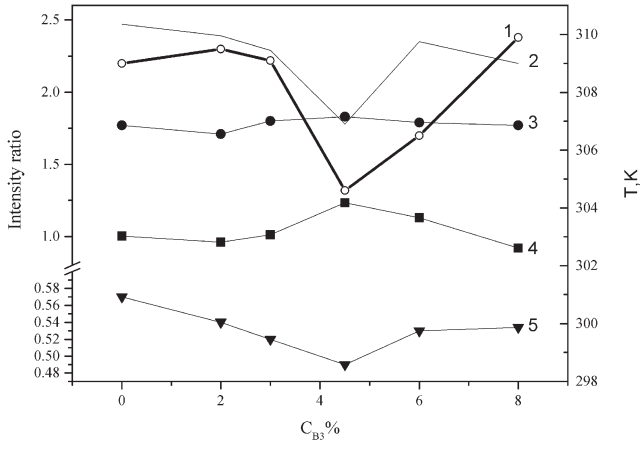

Figure 7. Dependence of PTT on B3 concentration (curve 1, right hand scale); and the relative intensities of the IR bands: curves 2, 3026/3070; 3, 2857/2928; 4, 1180/1186; 5, 2871/2957 cm^{-1}.

4. Conclusions

The effects of MMT organoclay (B3) concentration (2–8 wt%) on the structure formation and character of interactions between the components in 5CB–B3 nanocomposites have been investigated by XRD, IR-spectroscopy, POM and DSC methods. The modification of Na-MMT clay by the organic DODM was shown to cause a significant increase of interplanar distances in the clay structure. In the composites, 5CB dimers can penetrate into the interlayer spaces of the organoclay, additionally enlarging them. All experimental data indicate that the strongest (Van der Waals) interactions occur in the 5CB–B3 composites with C_{B3}=4.5 wt%. The structure of this composite is the most homogeneous.

Acknowledgements

This work was supported in part by Project NVC 5/06-N. The authors would like to thank Dr V. Moraru for the preparation of clay and composite samples and V. Nesprava for her help in this work.

References

[1] A. Glushchenko, H. Kresse, V. Reshetnyak, Yu, Reznikov, O. Yaroshchuk. *Liq. Cryst*, **23**, 241 (1997).
[2] S. Zakrevska, Yu, Zakrevskyy, A. Nych, O. Yaroshchuk, U. Mashke. *Mol. Cryst. liq. Cryst*, **375**, 467 (2002).
[3] B. Zhou, G. Iannacchione, C. Garland, T. Bellini. *Phys. Rev. E*, **55**, 2962 (1997).
[4] M. van Boxtel, M. Wubbenhorst, J. van Turnhout, C. Bastiaansen, D. Broer. *Liq. Cryst*, **30**, 235 (2003).
[5] S. Ponomarenko. PhD thesis, University of Kiev, Ukraine (2005) (in Ukrainian).
[6] T. Jones. *Clay Minerals*, **18**, 399 (1983).
[7] J. Feller, S. Bruzaud, Y. Grohens. *Mater. Lett*, **58**, 739 (2004).
[8] T. Bezrodna, I. Chashechnikova, L. Dolgov, G. Puchkovska, Ye, Shaydyuk, N. Lebovka, V. Moraru, J. Baran, H. Ratajczak. *Liq. Cryst*, **32**, 1005 (2005).
[9] G. Luckhurst, R. Stephans, R. Phyppen. *Liq. Cryst*, **8**, 451 (1990).
[10] P. Konarev, V. Volkov, A. Sokolova, M. Koch, D. Svergun. *J. Appl. Cryst*, **36**, 1277 (2003).
[11] C. Casewit, K. Colwell, A. Rappe. *J. Am. Chem. Soc*, **114**, 10035 (1992).
[12] G. Beaucage. *J. Appl. Cryst*, **29**, 134 (1996).
[13] F. Mercuri, A. Ghosh, M. Marinelli. *Phys. Rev. E*, **60**, 6309 (1999).
[14] M. Marinelli, A. Ghosh, F. Mercuri. *Phys. Rev. E*, **63**, 61713 (2001).
[15] A. Lazarev. *Vibrational Spectra and the Structure of Silicates* Nauka, Leningrad (1968) (in Russian).
[16] Tarasevich Yu, F. Ovchrenko. *Adsorption on the Clay Compounds* Naukova dumka, Kiev (1975) (in Russian).
[17] L. Babkov, I. Gnatyuk, G. Puchkovskaya, S. Truhachev. *J. Strukt. Chimii* **43**: 1098 (in Russian). (2002).
[18] K. Ishizaki, K. Matsushige. *Thin Solid Films*, **214**, 99 (1992).